

Novel SiO_x-coated carbon nanotubes

M. Rühle^{a,*}, T. Seeger^a, Ph. Redlich^a, N. Grobert^b, M. Terrones^{a,c}, D.R.M. Walton^b and H.W. Kroto^b

^aMax-Planck-Institut für Metallforschung, Seestraße 92, 70174 Stuttgart, Germany

^bUniversity of Sussex, CPES, The Fullerene Science Centre, Brighton BN1 9JQ, UK

^cInstituto de Física, UNAM, Laboratorio Juriquilla, Apartado Postal 1-1010, 76000 Querétaro, Qro., México

A room temperature colloidal method for coating carbon nanotubes with silicon oxide is described. Morphology, chemical composition and SiO_x/C interfaces of the coatings were investigated using state-of-the-art transmission electron microscopy and high spatially resolved electron energy-loss spectroscopy. The amorphous SiO_x coatings exhibit a thickness of up to 10 nm. In addition, coatings were also created by a high temperature route. However, they tend to be more unstable and spallate when compared to coatings deposited at room temperature.

Key words: Carbon nanotubes, Coating, SiO_x, HRTEM, HREELS.

Introduction

Carbon nanotubes (CNTs) are predicted to reinforce novel composite materials because of their structural perfection, excellent mechanical properties and low density [1-4]. In fibre-reinforced composites, the properties of the interface between the fibre and the matrix is crucial for the mechanical performance and structural integrity of the composite [5]. Therefore, the surface modification of CNT plays an important role in their use in composites. In this context, two main strategies for modifying CNTs' surface have been recently investigated: chemical modification of the outer walls [6-9] and coating with metals and metaloxides [10-14].

In this paper a room temperature method for coating multi-walled carbon nanotubes (MWNTs) with SiO_x using a sol-gel technique is described. SiO_x-coatings for CNTs by a high-temperature route, similar to the approach of Satishkumar *et al.* [15], were also prepared. The SiO_x coatings and C-SiO_x interfaces (present within the coated CNTs) were characterised by state of the art transmission electron microscopy (TEM) and high spatially resolved electron energy-loss spectroscopy (HREELS).

Experimental

For both processes, MWNTs produced by the standard arc-discharge technique [16] and tetraethoxysilane (TEOS) as the SiO_x precursor were used.

The high temperature coating route leads to adsorption of TEOS on the CNT surface and to subsequent decomposition at elevated temperature ($T \geq 230^\circ\text{C}$) [15]. In order to achieve this a MWNT-dispersion in TEOS (99.8%) was agitated for 24 h in the sonication bath. Residual

TEOS was then decanted and the powder remaining was annealed under an Ar atmosphere at 1000°C for 4 h.

The room temperature route is based on the creation of positive charges on the MWNTs surface by adsorption of the polyelectrolyte polyethylamine (PEI) and subsequent deposition of negatively charged colloidal SiO_x on the MWNT-surface [17, 18].

The coating process steps are as follows: CNTs (20 mg) were dispersed in a 0.25% PEI ($M_w=1200$) aqueous solution (100 cm³) and sonicated in a bath for 24 h. Residual PEI was removed by centrifugation (5000 min⁻¹, 4 h) and the sediment was redispersed in water for 1-2 min. This process was repeated twice. A mixture of TEOS, H₂O (pH 6) and ethanol (mass ratio 2 : 1 : 4) was set aside at room temperature for 48 h in order to achieve sol formation [19]. Then the CNT dispersion (step 1) and sol (step 2) were mixed in a 5 : 1 mass ratio. After 10 h of ultrasonic agitation (Bandelin Sonorex, 80 W/135 kHz) the mixture was homogenous and deposition of sol particles on the positively charged MWNTs occurred. After 100 h the material was washed with ethanol and subsequently centrifuged.

Samples were prepared for TEM by placing a drop of the nanotube/EtOH dispersion on a holey carbon TEM grid. Conventional TEM was performed on a Hitachi 7100 operating at 120 kV, high resolution TEM (HRTEM) on a JEOL 4000 EX operating at 400 kV and EELS using a GATAN DigiPEELS 766 on a dedicated STEM

*Corresponding author:
Tel: +49-711-2095318
Fax: +49-711-2095320
E-mail: ruehle@hrem.mpi-stuttgart.mpg.de

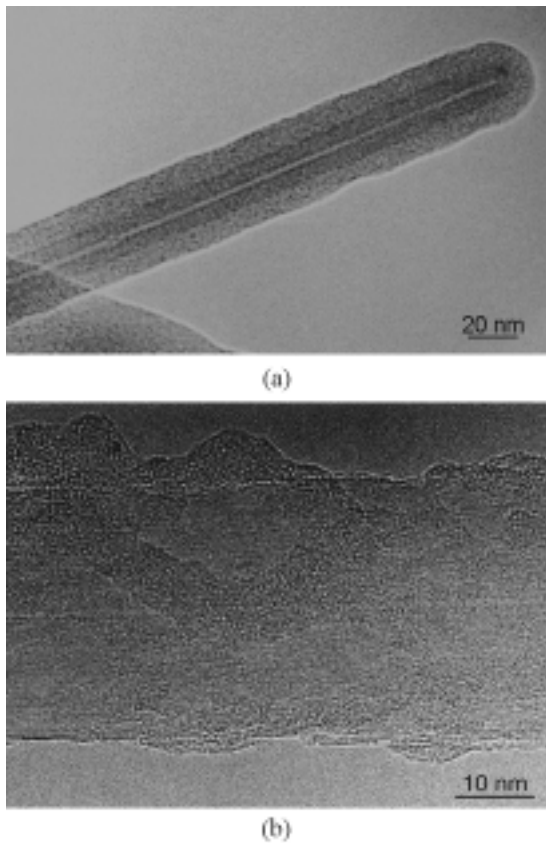


Fig. 1. SiO_x-coated CNT produced at high temperature: (a) low magnification TEM micrograph; uniform thickness *ca.* 10 nm; (b) HRTEM micrograph: coating several nm thick. Large areas of the nanotubes are not coated.

VG HB 501UX operating at 100 kV. Line scans were recorded by rastering the electron beam across the tube axis in 2 nm steps, measuring the EEL-spectrum for each step.

Results and Discussion

The high-temperature process results in CNTs with *ca.* 10 nm thick coatings, which appear to be uniform in conventional TEM micrographs (Fig. 1a). However, the HRTEM image of the same sample (Fig. 1b) taken several weeks after that shown in Fig. 1a reveals an incomplete surface coverage of the nanotube coating. Except for one surface step, the nanotube surface is still atomically smooth and does not show any interfacial layers. The elemental distribution profiles (Fig. 2a) are in agreement with our HRTEM results. In this case, silicon and oxygen can only be detected on one side of the CNT. For the positions marked in Fig. 2a (arrows), the Si L-edge spectra are compared (Fig. 4b). Spectrum 1 corresponds to the outer surface of the coating and spectra 2, 3 and 4 to positions located successively towards the coating/nanotube interface. Spectrum 1 exhibits maxima at 108 and 115 eV and an edge threshold at (103 ± 0.5) eV. In contrast to the other

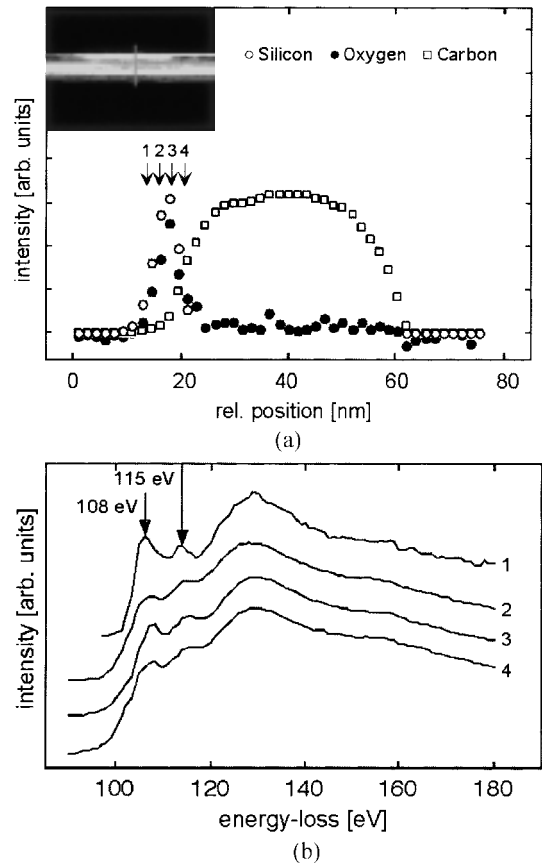


Fig. 2. SiO_x-coated CNT produced at high temperature: (a) EELS line scan of coated CNTs for Si, O and C. Rastered region marked on the inset of the dark field electron micrograph. Only one part of the nanotube is covered. In the central region of the tube the plasmon intensity was overlapping with the Si-L edge. Therefore the data for Si are not shown. Arrows mark the corresponding ELNES (Fig. 4b); (b) ELNES of the Si-L edge for different locations in the coating (arrows Fig. 4a). Except for spectrum 1 the ELNES does not change significantly for different locations.

spectra, the 108 eV peak is more prominent than that at 115 eV. Spectra 2, 3 and 4 are similar and exhibit a threshold energy of (100 ± 0.5) eV, a gradual increase of the intensity between 100 and 104 eV and two peaks at 108 eV and 115 eV.

Figure 3a shows a low magnification TEM micrograph of CNTs coated according to the room temperature scheme. The coating, 3-10 nm thick, covers the entire nanotube surface as shown in the HRTEM micrograph (Fig. 3b). The image contrast of the coatings shows an amorphous structure. However, in some parts of the coating (white arrow and inset) nanocrystallites have formed. The fringe spacing of these crystallites was found to be 0.30 ± 0.02 nm using the $\{0002\}$ spacing of the CNTs as internal reference. This spacing corresponds to that of the $\{111\}$ planes in Si. No interfacial layer could be detected between the coating and the nanotube surface.

The elemental distribution profiles derived from the EELS line scan analysis across CNTs, coated at room

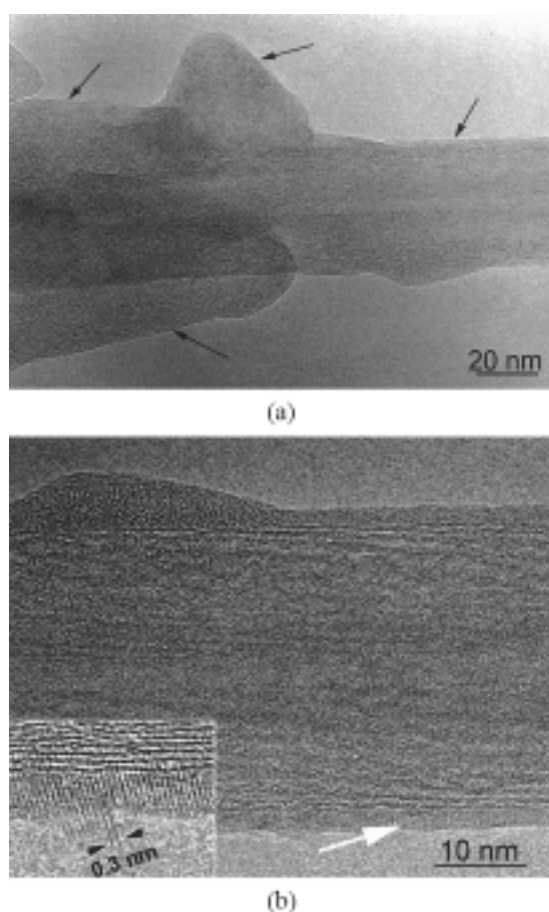


Fig. 3. SiO_x-gel coating for the low-temperature route: (a) low magnification TEM micrograph of a coated (arrows) MWNTs and polyhedral particles; (b) HRTEM micrograph of another coated CNT. The {0002}-graphite planes (0.34 nm spacing) are clearly visible. The coating (3 nm thick) is uniform over a wide area; however fluctuations in the deposition lead to local thickening. At the lower edge an arrow marks a crystalline region within the coating (for close-up see inset). The fringe spacing, (0.30 ± 0.02) nm, corresponds to the {111} planes of silicon.

temperature, are shown in Fig. 4a. The silicon and oxygen profiles match and show peaks on both sides of the nanotube, corresponding to the SiO_x coating. The CNT carbon intensity dominates the centre of the profiles. For locations marked in Fig. 4a (arrows 1 and 2), the Si-L edge spectra are plotted in Fig. 4b. The near edge fine structure (ELNES) reveals changes in the bonding and coordination of silicon, depending on the location.

Spectrum 1 of the outer coating surface exhibits an energy threshold at an energy-loss of (100 ± 0.5) eV. The edge onset for spectrum 2 measured in the SiO_x/CNT interface, is shifted to (104 ± 0.5) eV and exhibits distinct maxima at 108 and 115 eV, which indicate the presence of the “SiO₄” tetrahedron [20]. It is clear that these almost not detectable in the outer coating surface.

The above observations show that the room and high-temperature methods result in very different coating

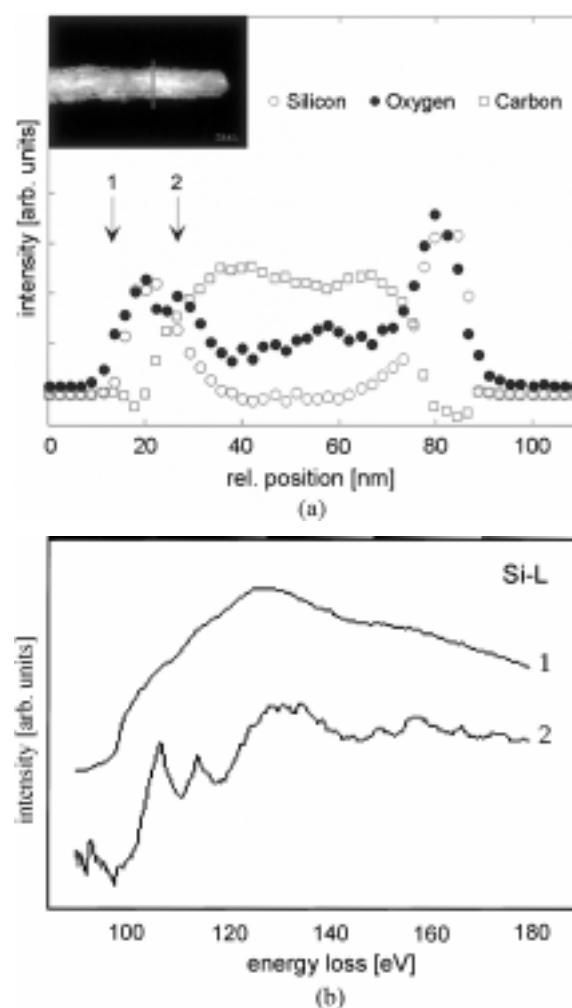


Fig. 4. SiO_x-gel coating for the low-temperature route: (a) EELS linescan over a SiO_x-coated CNT. The rastered region is marked on the inset of the dark field electron micrograph. Si and O coat the whole surface. The arrows mark the corresponding ELNES of Fig. 2b. The low amount of Si measured in the central region of the tube results from overlap of the Si-L edge and the plasmon-peak which becomes intense for thick specimens; (b) ELNES of the Si-L edge for two different locations in the coating (arrows in Fig. 2a). The ELNES changes for different locations in the coating indicating variations in O content.

morphologies. Direct TEOS deposition and subsequent high-temperature annealing generates highly regular coatings (Fig. 1a). However, these coatings spallate spontaneously with time (Fig. 1b). The sol-gel room temperature technique leads to stable coatings for CNTs (Figs. 3a-c).

Information regarding the chemical character of coatings derived from ELNES of the Si-L edge can be used to obtain additional data about the bonding within the SiO_x coating and the SiO_x-C interface. The Si-L ELNES of SiO_x has been investigated by various authors: Batson [20] showed that an ELNES with maxima at 108 eV, 115 eV and an excitonic shoulder at 106 eV are likely to characterize “SiO₄” bonding units. In addition, a slope that extends from the oxide excitonic peak down to 99.8 eV arises from an oxide

with SiO stoichiometry. Dori *et al.* [21] investigated silicon-rich oxide layers and attributed this slope to Intermediate bonding states of silicon (Si^{3+} , Si^{2+} , Si^{+}) as well as to a superposition of the pure SiSi_4 (energy threshold: 99.8 eV) and the “ SiO_4 ” bonding unit spectra. Chen *et al.* [22] measured the Si-L ELNES of SiO_2 during electron irradiation and detected a decrease of the maxima at 108 and 115 eV, due to oxygen depletion, which suggests formation of an irradiation-induced substoichiometric oxide. These authors also observed formation of amorphous silicon as a result of electron irradiation. For the sol-gel room temperature coating, the Si-L ELNES at the coating/nanotube interface (spectrum 2; Fig. 4b) reveals formation of SiO_2 with maxima at 108 and 115 eV, and an excitonic shoulder at 106 eV [20]. No contribution indicating an interface reaction, such as carbide formation (which is not expected for a room temperature process) could be detected. The energy shift in the spectrum 1 (closer to the outer coating surface, Fig. 4b) can be attributed to the presence of more substoichiometric SiO_x . At the same time, the almost extinguished peaks located at 108 and 115 eV indicate a considerable loss of oxygen, which is possibly due to electron irradiation during the measurements. The pronounced effect of the electron beam during measurements in the outer regions can be due to either the electron dose per SiO_x -subunit being smaller in the outer regions due to the coating geometry, or to the internal structure of the coating which is less cross-linked. The latter argument could lead to relevant information about the coating mechanism. The possibility of generating silicon by the electron beam accounts for the formation of silicon nanocrystals found in the room temperature coating (Fig. 3b). Takeguchi *et al.* [23] produced nanocrystalline Si in SiO_2 in a 200 kV electron microscope using a heating stage at 580°C. The 400 keV electrons and the still imperfect SiO_x -network in our sample have obviously overcompensated for the lack of external heating for the Si nanocrystal formation.

For the coatings produced at high temperature, Si-L ELNES spectra 1, 2, 3 and 4 (Fig. 2c) are characteristic of substoichiometric SiO_x and show - in comparison with the room temperature coating - less degradation in dependence of the location in the coating. This suggests that the high temperature generated coatings are more resistant to electron beam degradation, indicating that annealing at 1000°C leads to a stable silicon oxide network. The slight oxygen depletion within the coatings does not seem to originate from electron irradiation effects. However, spontaneous spallation of the coating is likely to arise from this brittle network, which tends to fracture due to mechanical stress. By contrast, the sol-gel derived coatings prepared at room temperature contain a less dense oxide which retains more flexibility and crack resistance.

Conclusions

Silicon oxide coatings have been generated on the surface of arc-grown MWNT₅ by a high temperature route and at room temperature involving a sol-gel technique. HRTEM and EELS studies revealed the absence of interface reactions between the coating and the CNTs. The room temperature process appears to produce uniform coatings, which appear to be less stable under the electron beam when compared to those produced at high temperature.

Finally, we observed that electron beam irradiation can also be used to form silicon nanocrystals on the surface of the carbon nanotube by decomposition of the silicon oxide. Considering recent results of Shatishkumar and coworkers [14], the influence of charging CNT by a polelectrolyte prior to coating deposition should be investigated in detail.

Acknowledgements

We thank the DFG (Contract No.: Ru 342/11-2) for financial support.

References

1. B.I. Yakobson, C.J. Brabec, and J. Bernholc, *Phys. Rev. Lett.* 76 (1996) 2511.
2. J.P. Lu, *Phys. Rev. Lett.* 79 (1977) 1297.
3. E.W. Wong, P.E. Sheehan, and C.M. Lieber, *Science* 277 (1997) 1971.
4. O. Lourie, D.M. Cox, and H.D. Wagner, *Phys. Rev. Lett.* 81 (1998) 1638.
5. J.-K. Kim, and J.-W. Mai, in *Materials Science and Technology*, (Eds. R.W. Cahn, P. Haasen, E.J. Kramer), Vol. 13: Structure and Properties of composites, (Ed. T.W. Chou, VCH Weinheim 1993).
6. T.W. Ebbesen, *J. Phys. Chem. Solids* 57 (1996) 951.
7. T. Nakajima, S. Kasamatsu, and Y. Matsuo, *European Journal of Solid State & Inorganic Chemistry* 33 (1996) 831.
8. E.T. Mickelson, C.B. Huffman, A.G. Rinzler, R.E. Smalley, R.H. Hauge, and J.L. Margrave, *Chem. Phys. Lett.* 296 (1998) 188.
9. P.J. Boul, J. Liu, E.T. Mickelson, C.B. Huffman, L.M. Ericson, I.W. Chiang, K.A. Smith, D.T. Colbert, R.H. Hauge, J.L. Margrave, and R.E. Smalley, *Chem. Phys. Lett.* 310 (1999) 367.
10. P.M. Ajayan, O. Stephan, P. Redlich, and C. Colliex, *Nature* 375 (1995) 564.
11. B.C. Satishkumar, E.M. Vogl, A. Govindaraj, and C.N.R. Rao, *J. Phys. D - Appl. Phys.* 29 (1996) 317.
12. Q.Q. Li, S.H. Fan, W.Q. Han, C.H. Sun, and W.J. Liang, *Japan. J. Appl. Phys.* p.2-Lett. 36 (1997) L 501.
13. X.H. Chen, J.T. Xia, J.C. Peng, W.Z. Li, and S.S. Xie, *Composites Science & Technology* 60 (2000) 301.
14. B.C. Satishkumar, A. Govindaraj, Manashi Nath, C. N. R. Rao, *J. Mater. Chem* 10 (2000) 2115
15. B.C. Satishkumar, A. Govindaraj, E.M. Vogl, L. Basumallick, and C. N. R. Rao, *J. Mater. Res.* 12 (1997) 604.
16. T.W. Ebbesen, and P.M. Ajayan, *Nature* 358 (1992) 220.

17. B. Alince, J. Petlicki, and T.G.M. Vandeven, *Colloids and Surfaces* 59 (1991) 265.
18. S. Suty, and V. Luzakova, *Colloids and Surfaces, A - Physicochemical and Engineering Aspects* 139 (1998) 271.
19. C.J. Brinker, and G.W. Scherer, in *Sol - Gel Science*, Academic Press, San Diego 1990.
20. P.E. Batson, *Microsc. Microanal. Microstruct* 2 (1991) 395.
21. L. Dori, J. Bruley, D.J. DiMaria, P.E. Batson, J. Tornello, and M. Arienzo, *J. Appl. Phys.* 69 (1991) 2317.
22. G.S. Chen, C.B. Boothroyd, and C.J. Hymphreys, *Appl. Phys. Lett.* 62 (1993) 1949.
23. M. Takeguchi, K. Furuya, and K. Yoshihara, *Micron* 30 (1999) 147.